

Noninvasive CT radiomic model for preoperative prediction of lymph node metastasis in early cervical carcinoma

Short title: CT radiomic model for lymph node metastasis.

Type of Manuscript: Full paper.

Authors: Jiaming Chen^{1,2#}, Bingxi He^{3,4,5#}, Di Dong^{3,5#}, Ping Liu^{1,2}, Hui Duan^{1,2}, Weili Li^{1,2}, Pengfei Li^{1,2}, Lu Wang^{1,2}, Huijian Fan^{1,2}, Siwen Wang^{3,5}, Liwen Zhang^{3,5}, Jie Tian^{3,5,6*}, Zhipei Huang^{4,5*}, Chunlin Chen^{1,2*}

(# Jiaming Chen, Bingxi He, and Di Dong contributed equally to this work)

Author affiliations :

1 Department of Obstetrics and Gynecology, Nanfang Hospital, Southern Medical University, Guangzhou, China

2 Digital Medical Laboratory of Department of Obstetrics and Gynecology, Nanfang Hospital, Southern Medical University, Guangzhou, China

3 CAS Key Laboratory of Molecular Imaging, Institute of Automation, Chinese Academy of Sciences, Beijing, China

4 School of Electronic, Electrical and Communication Engineering, University of Chinese Academy of Sciences, Beijing, China

5 University of Chinese Academy of Sciences, Beijing, China

6 Beijing Advanced Innovation Center for Big Data-Based Precision Medicine,
Beihang University, Beijing, China

***Corresponding Authors:**

Jie Tian, Department of CAS Key Laboratory of Molecular Imaging, Institute of Automation, Chinese Academy of Sciences, No 95, Zhongguancun East Road, Beijing 100190, China; Email: jie.tian@ia.ac.cn; Tel: +86 10 82618465; Fax: +86 10 62527995

Zhipei Huang, School of Electronic, Electrical and Communication Engineering, University of Chinese Academy of Sciences, Beijing 101408, China; Email: zhphuang@ucas.ac.cn; Tel: +86 10 69671882

Chunlin Chen, Department of Obstetrics and Gynecology of Nanfang Hospital, Guangzhou, Guangdong, China; Email: ccl1@smu.edu.cn Tel: +86 13725263051

Conflict of interest statement: No.

Acknowledgments: We would like to express our gratitude for financial support from the National Key R&D Program of China (2017YFC1308700, 2017YFA0205200, 2017YFC1309100, 2017YFC1308701, 2016YFC0103803, 2017YFA0700401), the National Natural Science Foundation of China (81571422, 81370736, 81771924, 81501616, 81227901, 81671851, 81527805, 61671449, 61622117), the National

Science and Technology Support Program of China (2014BAI05B03), the National Natural Science Fund of Guangdong (2015A030311024), the Science and Technology Plan of Guangzhou (158100075), the Beijing Municipal Science and Technology Commission (Z171100000117023, Z161100002616022), the Instrument Developing Project of the Chinese Academy of Sciences (YZ201502), and the Youth Innovation Promotion Association CAS (2017175).

Abstract

Rationale and Objectives

To build and validate a computed tomography (CT) radiomic model for preoperatively predicting lymph node metastasis in early cervical carcinoma.

Materials and Methods

A dataset of 150 patients with stage IB1 to IIA2 cervical carcinoma was retrospectively collected from the xx and separated into a training cohort (n = 104) and test cohort (n = 46). A total of 348 radiomic features were extracted from the delay phase of CT images. Mann-Whitney U test, recursive feature elimination, and backward elimination were used to select key radiomic features. Ridge logistics regression was used to build a radiomic model for prediction of lymph node metastasis (LNM) status by combining radiomic and clinical features. The area under the receiver operating characteristic curve (AUC) and kappa test were applied to verify the model.

Results

Two radiomic features from delay phase CT images and one clinical feature were

associated with LNM status: log-sigma-2-0-mm-3D_glcmln (P = 0.01937), wavelet-HL_firstorder_Median (P = 0.03592), and stage IB (P = 0.03608). Radiomic model was built consisting of the three features, and the AUCs were 0.80 (95% confidence interval (CI): 0.70~0.90) and 0.75 (95%CI: 0.53~0.93) in training and test cohorts, respectively. The kappa coefficient was 0.84, showing excellent consistency.

Conclusions

A noninvasive radiomic model, combining two radiomic features and a FIGO stage, was built for prediction of LNM status in early cervical carcinoma. This model could serve as a preoperative tool.

Advances in knowledge

A noninvasive CT radiomic model, combining two radiomic features and the FIGO stage, was built for prediction of LNM status in early cervical carcinoma.

Noninvasive CT radiomic model for preoperative prediction of lymph node metastasis in early cervical carcinoma

Short title: CT radiomic model for lymph node metastasis.

Abstract

Rationale and Objectives

To build and validate a computed tomography (CT) radiomic model for preoperatively predicting lymph node metastasis in early cervical carcinoma.

Materials and Methods

A dataset of 150 patients with stage IB1 to IIA2 cervical carcinoma was retrospectively collected from the xx and separated into a training cohort ($n = 104$) and test cohort ($n = 46$). A total of 348 radiomic features were extracted from the delay phase of CT images. Mann-Whitney U test, recursive feature elimination, and backward elimination were used to select key radiomic features. Ridge logistics regression was used to build a radiomic model for prediction of lymph node metastasis (LNM) status by combining radiomic and clinical features. The area under the receiver operating characteristic curve (AUC) and kappa test were applied to verify the model.

Results

Two radiomic features from delay phase CT images and one clinical feature were associated with LNM status: log-sigma-2-0-mm-3D_glcmln ($P = 0.01937$), wavelet-HL_firstorder_Median ($P = 0.03592$), and stage IB ($P = 0.03608$). Radiomic model was

built consisting of the three features, and the AUCs were 0.80 (95% confidence interval (CI): 0.70~0.90) and 0.75 (95%CI: 0.53~0.93) in training and test cohorts, respectively.

The kappa coefficient was 0.84, showing excellent consistency.

Conclusions

A noninvasive radiomic model, combining two radiomic features and a FIGO stage, was built for prediction of LNM status in early cervical carcinoma. This model could serve as a preoperative tool.

Advances in knowledge

A noninvasive CT radiomic model, combining two radiomic features and the FIGO stage, was built for prediction of LNM status in early cervical carcinoma.

Introduction

Cervical carcinoma is a common malignant tumor, with an annual worldwide incidence of 500,000, more than 80% of which are in developing countries (1). In China, the incidence and mortality of cervical carcinoma are 98,900 and 30,500 in 2015, respectively (2).

Surgery and adjuvant therapy are the main therapy options for cervical carcinoma.

Lymph node metastasis (LNM) is an independent risk factor for the outcome of cervical carcinoma, and pelvic lymphadenectomy (PLD) is routinely recommended during surgery, which is required for cervical carcinoma with International Federation of Gynecology and Obstetrics (FIGO) stage IA1 with LVSI and stage IA2 to IIA2 (3).

Previous studies reported that no more than 30% of early cervical carcinoma patients had LNM (4–7), which suggests that 70% of patients underwent unnecessary PLD, and some even underwent unnecessary lymph node (LN) radiotherapy. Such overtreatment is caused by inaccurate LNM staging before surgery. The gold standard for LNM staging is postoperative histology. However, a surgeon needs to dissect important vessels, which is associated with high difficulty, high risk, and a series of intraoperative and postoperative complications (8–11). Preoperative diagnosis of LNM is mainly dependent on computed tomography (CT) and magnetic resonance imaging (MRI) based on the morphology of LN, which suffers from great subjectivity (12–14).

Therefore, new methods for accurate diagnosis of LNM before surgery are needed to help doctors establish personalized PLD schedules.

Recently, radiomics has been proposed to extract rich information by quantitative and

high throughput analysis of conventional medical images (15,16). It has been used to estimate LNM status by extracting quantitative characteristics from CT images related to bladder, colorectal, breast, thyroid, esophageal, and lung adenocarcinoma, and the radiomics nomogram showed good predictive performance (17–23). Therefore, the intention of this study was to assess the LNM status in individuals affected by cervical carcinoma by using a CT radiomics method. To accomplish this, we developed a radiomic model to obtain predictions of the LNM status preoperatively.

Materials and Methods

Patients

This was a retrospective study, and requirement for patients' informed consent was waived by the institutional review board of our hospital. We reviewed records from between 2008 and 2018. Considering the longest time required for the effects of the drugs to be apparent in CT images, the experiments were performed first on patients with a delay phase. A total of 172 cervical carcinoma cases with a FIGO stage from IB1 to IIA2 were included in accordance with the following criteria: 1. postoperative histology confirmed cervical carcinoma and LN status; 2. no preoperative adjuvant therapy; 3. preoperative CT images (thickness of 1.0 mm or 1.5 mm) and available clinical data; 4. no other malignant tumors; 5. patients with complete delay phase CT images. Twenty-two patients were excluded for the following criteria: 1. maximum diameter of the tumor was less than 20 pixels; 2. metal artifacts exist in images. Finally, 150 patients with delay phase CT scans were enrolled and sorted by CT acquired time;

the first 70% of the patients were used as the training cohort (n=104, containing 21 LNM patients and 83 non-LNM patients), the remainder as the test cohort (n=46, containing 10 LNM patients and 36 non-LNM patients).

Clinical and Pathologic Features

Clinical, imaging, and pathological information were collected from the hospital system (DHC-EMR; Table 1). Clinical features included age, menarche time, pregnancy and parturition numbers, FIGO stage, and histological type of tumor. Imaging features included the status of corpus uteri, vagina, and LN on CT reports. Pathological information included the status of LNM after surgery.

CT Image Acquisition

All patients were scanned by the SIEMENS Definition Double Source CT (SOMATOM Definition, Siemens Ltd, Germany). Scanning range was from the upper margin of the kidney to 2 cm off the lower edge of the pubic symphysis. We used a double tube high pressure syringe at a speed of 3.5 ml/s to engage patients with a right cubital vein injection of 75 ml non-ionic iodine contrast agent Ultravist (370mgL/mL, Schering Pharmaceutical Co. Ltd. Guangzhou Germany), followed with 30 ml normal saline. At the same time, aortic bifurcation 2.0 cm above the region of interest (ROI) was performed using contrast tracer method (BOLUS TRACKING) dynamic monitoring of CT; an automatic trigger scan ROI was setup when the CT value reached 120 Hu. After 35 s priming delayed venous phase scanning and 120 s trigger delayed phase scanning,

venous phase and delayed phase image capture were performed, respectively. All images were derived in the DICOM3.0 format.

Tumor Segmentation

ROI segmentation was indispensable for feature extraction. One gynecologist with 5 years of experience (observer 1) manually delineated two-dimensional ROI (the largest area of the primary tumor) on all original images of plain scan, arterial phase, venous phase, and delayed phase, using the ITK-SNAP open-source software (www.itk-snap.org). Another gynecologist with 10 years of experience (observer 2) examined all the segmentations. Observer 2 selected 30 cases randomly and re-delineated the ROIs to test the inter-observer error.

Radiomic Feature Extraction

We obtained a series of CT scans with mean values of 0 and variance of 1 by using z-score method in the training cohort, and then resampled these CT scans to ensure that each scan had the same layer to layer and voxel to voxel spacing.

Then, two-dimensional radiomic features were extracted from the ROIs. Image transformation used two types of filters (Fig. 1): (I) Wavelet filter, and (II) Laplacian of Gaussian (LOG) filter. The radiomic features were divided into three groups: (I) first-order statistical features, (II) morphological features, and (III) texture features. The explanations of radiomics features and image filters are detailed in Supplement 1.

Statistical Analysis

For the LNM class, we used label encoding to represent discrete properties in terms of numbers, and binarized these numbers by one-hot encoding. Apart from making features sparse, one-hot encoding can also add the number of features. The output of the model is the probability of LNM.

The Mann-Whitney U test was used to examine the significance of radiomic features (P value < 0.05 was considered significant). To eliminate redundant features with collinearity, we carried out recursive feature elimination (RFE) with cross-validation. RFE is a greedy algorithm for finding a preferable feature subset; the underlying RFE model used here was ridge logistic regression. We choose backward elimination to identify optimum feature combination by adding all variables to the regression equation at one time and then sequentially removing single variable that did not significantly affect the regression equation until all variables were significant. What needs to be added is that the multivariate P value < 0.05 indicates that the effect on the regression equation is significant.

Logistic regression with L2-norm was used to construct the radiomic model. Owing to the unbalanced samples, class weights were adjusted. Model performance was assessed by the receiver operating characteristic (ROC) curve and the area under the curve (AUC). At the same time, we also used a calibration curve to evaluate the model.

Decision curve analysis helps choose the model that predicts the greatest net benefit.

The abscissa indicates the threshold probability and the ordinate indicates the net benefit. The higher the decision curve, the better the model's net income. Furthermore,

we performed an inter-observer error test on segmentation results from the 30 selected patients and calculated the kappa coefficient between the two results (kappa coefficient > 0.6 indicates a feature with high consistency).

We used Python (URL: <https://www.python.org/>, version 3.6.5) to extract features and perform statistical analysis (Fig. 2). The 'pyradiomics' package was used to extract radiomics features. The 'scikit-learn' package was applied for RFE, cross-validation, ridge logistic regression, and model evaluation.

Results

Clinical Features and Radiomic Features

This study contained 150 patients (104 in the training cohort and 46 in the test cohort). The mean age were 47.87 ± 10.61 and 45.80 ± 13.72 in the training cohort and test cohort, respectively. Seventy-seven patients of IB stage and 27 patients of IIA stage were in the training cohort, and 38 patients of IB stage and 8 patients of IIA stage were in the test cohort. Squamous carcinoma and non-squamous carcinoma in the training and test cohort were 82 and 21, and 38 and 6, respectively. Fifteen and 5 patients were reported LNM by CT in the training and test cohort. We extracted 348 radiomic features from the tumor ROI, including 108 first-order statistical features, 12 morphological features, and 232 texture features.

As shown in Fig. 3, the performance (accuracy) of the model was best when the number of features was 10. In light of the backward elimination results, three features were selected for modeling: (1) log-sigma-2-0-mm-3D_glcmln (Inverse Difference

1 Normalized), representing the local homogeneity of the CT after using the LOG filter;
2
3 (2) wavelet-hl_firstorder_median, representing the median gray level intensity in the
4
5 ROI after using the wavelet filter (HL); (3) stage IB, representing that the patient's
6
7 FIGO stage was IB. The P values in multivariate analysis were less than 0.0001. The
8
9 distribution of these features is shown in Fig. 3.
10
11
12
13
14
15
16

17 ***Apparent Performance of the Radiomics Model***

18
19 We used the three selected features to build a radiomics model, which was then applied
20
21 in the test cohort for testing. The ROC curves of the radiomic model in the training and
22
23 test cohorts are shown in Fig. 4. The AUCs of the radiomic model in the training and
24
25 test cohorts were 0.80 (95%CI: 0.70–0.90) and 0.75 (95%CI: 0.53–0.93), respectively,
26
27 indicating that the model was a good predictor of LNM. In addition, we removed
28
29 clinical features and only used radiomic features to build a model (AUC: 0.73 [95%CI:
30
31 0.60–0.85]; Fig. 4), and found that the addition of clinical features could significantly
32
33 improve the performance of the model. The decision curve of the radiomic model is
34
35 shown in Fig. 4. We found that when the threshold probability was larger than 5%, the
36
37 radiomic model was more effective than treat-all and treat-none schemes.
38
39
40
41
42
43
44
45
46
47
48
49

50 ***Validation of the Radiomics Model***

51
52 The result of the kappa test between the two segmentations (i.e., those performed by
53
54 the two observers) was 0.84, indicating excellent consistency of the features.
55
56
57

58 We further investigated the phases by supplementing 149 patients with arterial phase
59
60
61
62
63
64
65

and 146 patients with venous phase to implement the prediction of LNM. We found that there were no significant radiomics features for arterial phase patients and a non-significant prediction result for venous phase patients.

Discussion and Conclusion

We developed and validated a CT radiomic model for preoperative prediction of LNM in early cervical carcinoma. By the validation in the test set, we found that the radiomic model had good predictive capacity. This study tested radiomic and clinical features to establish the model, and three features were singled out: (1) log-sigma-2-0-mm-3D_glcmln_Idn (Inverse Difference Normalized); (2) wavelet-hl_firstorder_median; (3) stage IB.

The main preoperative techniques for predicting LNM are LN ultrasonography, CT, MRI, PET-CT, and needle aspiration biopsy of LN. Ultrasonography is only suitable for superficial LN, but is unsatisfactory for deep LN such as pelvic lymph nodes. CT and MRI are the most widely used imaging examinations for LN diagnosis. Criteria for determining LNM are based on morphology (e.g., shortest diameter more than 1 cm, uneven density of LN, central necrosis, coarse envelope, or shape of the circle from an ellipse). The sensitivity and specificity of CT and MRI in the diagnosis of LN are 64% & 72%, and 93% & 93%, respectively (12). These two methods have certain subjectivities, making it difficult to distinguish metastatic LN and inflammatory LN (12–14). Consequently, the evaluating performance is poor, and the diameters of metastatic LN with more than 40% are less than 1 cm (24,25).

Many hospitals lack PET-CT equipment, and the cost of inspection is very high; therefore, this approach is not widely used at present. Some researchers have suggested that the value of FDG-PET for LNM diagnosis is not as good as that using MRI, where sensitivity and specificity in detecting pelvic LN were 67% and 84% with MRI, and 33% and 92% with FDG-PET in their study (14,26).

The 2018 National Comprehensive Cancer Network clinical practice guidelines no longer recommend LN needle aspiration biopsy (3). Errors in preoperative molecular detection of solid tumors are spatially and temporally heterogeneous, but relatively noninvasive medical imaging examination could provide more comprehensive information (27).

The limitations of our study were as follows. First, all data were from a single center. Multi-center external validation with a larger sample size is needed to improve the predictive capacity of the model for clinical application. Second, we only identified the largest area of the primary tumor. Therefore, this study lacked three-dimensional radiomics analysis. Third, only CT data were used for radiomics analysis; it may be better to combine preoperative biopsy pathological images or MRI data to construct the model and that will be our future direction of work.

In conclusion, this radiomic model, which combined two radiomic features and FIGO stage, is a noninvasive tool that shows good performance. It could be potentially and conveniently used for assessing LNM status individually before surgery in early cervical carcinoma patients. Furthermore, the use of this model could avoid unnecessary PLD, which would reduce treatment risks and the financial burden of these

patients.

1
2
3
4
5
6
7
8
9
10
11
12
13
14
15
16
17
18
19
20
21
22
23
24
25
26
27
28
29
30
31
32
33
34
35
36
37
38
39
40
41
42
43
44
45
46
47
48
49
50
51
52
53
54
55
56
57
58
59
60
61
62
63
64
65

References

1. Tsu V, Jerónimo J. Saving the World's Women from Cervical Cancer. *N Engl J Med*. 2016 Jun 30;374(26):2509-11.
2. Chen WQ, Zheng RS, Baade PD, et. al. Cancer statistics in China, 2015. *CA Cancer J Clin*. 2016 Mar-Apr;66(2):115-32.
3. Koh, W. J, Aburustum, et. al. Uterine Neoplasms, Version 1.2018, NCCN Clinical Practice Guidelines in Oncology. *Journal of the National Comprehensive Cancer Network Jccn*, 2018, 16(2):170-199.
4. Sakuragi N, Satoh C, Takeda N, et. al. Incidence and Distribution Pattern of Pelvic and Paraaortic Lymph Node Metastasis in Patients with Stages IB, IIA, and IIB Cervical Carcinoma Treated with Radical Hysterectomy. *Cancer*. 1999 Apr 1;85(7):1547-54.
5. Martínez A, Mery E, Filleron T, Boileau L, Ferron G, Querleu D. Accuracy of intraoperative pathological examination of SLN in cervical cancer. *Gynecol Oncol*. 2013 Sep;130(3):525-9.
6. Ditto A, Martinelli F, Lo Vullo S, et. al. The role of lymphadenectomy in cervical cancer patients: the significance of the number and the status of lymph nodes removed in 526 cases treated in a single institution. *Ann Surg Oncol*. 2013 Nov;20(12):3948-54.
7. Du R, Li L, Ma S, Tan X1, Zhong S1, Wu M1. Lymph nodes metastasis in cervical cancer: Incidences, risk factors, consequences and imaging evaluations. *Asia Pac J Clin Oncol*. 2018 May 31.
8. Querleu D, Leblanc E, Cartron G, Narducci F, Ferron G, Martel P. Audit of preoperative and early complications of laparoscopic lymph node dissection in 1000 gynecologic cancer patients. *Am J Obstet Gynecol*. 2006 Nov;195 (5):1287-92.
9. Achouri A, Huchon C, Bats AS, Bensaid C, Nos C, Lécure F. Complications of lymphadenectomy for gynecologic cancer. *Eur J Surg Oncol*. 2013 Jan;39(1):81-6.
10. Musch M, Klevecka V, Roggenbuck U, Kroepfl D. Complications of pelvic lymphadenectomy in 1,380 patients undergoing radical retropubic prostatectomy

- between 1993 and 2006. *J Urol*. 2008 Mar;179(3):923-8.
11. Tanaka T, Ohki N, Kojima A, et. al. Radiotherapy negates the effect of retroperitoneal nonclosure for prevention of lymphedema of the legs following pelvic lymphadenectomy for gynecological malignancies: an analysis from a questionnaire survey. *Int J Gynecol Cancer*. 2007 Mar-Apr;17(2):460-4.
12. Kasuya G, Toita T, Furutani K, et. al. Distribution patterns of metastatic pelvic lymph nodes assessed by CT/MRI in patients with uterine cervical cancer. *Radiat Oncol*. 2013 Jun 8;8:139.
13. Pelikan HM1, Trum JW, Bakers FC, Beets-Tan RG, Smits LJ, Kruitwagen RF. Diagnostic accuracy of preoperative tests for lymph node status in endometrial cancer: a systematic review. *Cancer Imaging*. 2013 Jul 22;13(3):314-22.
14. Park JY, Lee JJ, Choi HJ, et. al. The Value of Preoperative Positron Emission Tomography/Computed Tomography in Node-Negative Endometrial Cancer on Magnetic Resonance Imaging. *Ann Surg Oncol*. 2017 Aug;24(8):2303-2310.
15. Lambin P, Leijenaar RTH, Deist TM, et. al. Radiomics: the bridge between medical imaging and personalized medicine. *Nat Rev Clin Oncol*. 2017 Dec;14(12):749-762.
16. Wang S, Shi J, Ye Z, et al. Predicting EGFR mutation status in lung adenocarcinoma on computed tomography image using deep learning. *Eur Respir J*. 2019;53(3):1800986.
17. Wu S, Zheng J, Li Y, et. al. A Radiomics Nomogram for the Preoperative Prediction of Lymph Node Metastasis in Bladder Cancer. *Clin Cancer Res*. 2017 Nov 15;23(22):6904-6911.
18. Huang YQ, Liang CH, He L, et. al. Development and Validation of a Radiomics Nomogram for Preoperative Prediction of Lymph Node Metastasis in Colorectal Cancer. *J Clin Oncol*. 2016 Jun 20;34(18):2157-64.
19. Zhong Y, Yuan M, Zhang T, Zhang YD, Li H, Yu TF. Radiomics Approach to Prediction of Occult Mediastinal Lymph Node Metastasis of Lung Adenocarcinoma. *AJR Am J Roentgenol*. 2018 Jul;211(1):109-113.
20. Shen C, Liu Z, Wang Z, et. al. Building CT Radiomics Based Nomogram for Preoperative Esophageal Cancer Patients Lymph Node Metastasis Prediction.

Transl Oncol. 2018 Jun;11(3):815-824.

21. Dong D, Tang L, Li ZY, et. al. Development and validation of an individualized nomogram to identify occult peritoneal metastasis in patients with advanced gastric cancer. *Ann Oncol.* 2019 Jan 23.
22. Dong Y, Feng Q, Yang W, et. al. Preoperative prediction of sentinel lymph node metastasis in breast cancer based on radiomics of T2-weighted fat-suppression and diffusion-weighted MRI. *Eur Radiol.* 2018 Feb;28(2):582-591.
23. Liu T, Ge X, Yu J, Guo Y, Wang Y, Wang W, Cui L. Comparison of the application of B-mode and strain elastography ultrasound in the estimation of lymph node metastasis of papillary thyroid carcinoma based on a radiomics approach. *Int J Comput Assist Radiol Surg.* 2018 Jun 21.
24. Aoki T, Tomoda Y, Watanabe H, et. al. Peripheral lung adenocarcinoma: correlation of thin-section CT findings with histologic prognostic factors and survival. *Radiology*, 2001,220(3):803-809.
25. Valls C, Andia E, Sanchez A, et. al. Dual-phase helical CT of pancreatic adenocarcinoma: assessment of resectability before surgery. *AJR*, 2002, 178(4):821-826
26. Monteil J, Maubon A, Leobon S, et. al. Lymph node assessment with (18)F-FDG-PET and MRI in uterine cervical cancer. *Anticancer Res.* 2011 Nov;31(11):3865-71.
27. Lambin P, Rios-Velazquez E, Leijenaar R, et. al. Radiomics: extracting more information from medical images using advanced feature analysis. *Eur J Cancer.* 2012 Mar;48(4):441-6..

Figure Legend

Fig. 1. Inclusion and exclusion criteria.

Fig. 2 Flow chart of statistical analysis.

Fig. 3 (a) showed the model performance evaluated through the numbers of features as a function of the cross-validation feature recursive elimination algorithm. (b), (c), (d) and (e) were statistical charts for the optimal subset of features. (b) and (c) were violin-plots of radiomic features in the training cohort and test cohort, respectively. (d) and (e) showed count-plots of clinical features in the training cohort and test cohort, respectively.

Fig. 4 (a) was the receiver operating characteristic (ROC) curve of radiomic models for the training cohort (red, green, and yellow lines) and test cohort (blue line). (b) was the decision curve for the radiomics model (red line), clinical model (green line), radiomics model only using radiomics features (yellow line), treat-all (thin black line), and treat-none (thick black line) schemes. The thin black line represented the assumption that all patients have lymph node metastasis (LNM); the thick black thick represented the assumption that none of the patients have LNM.

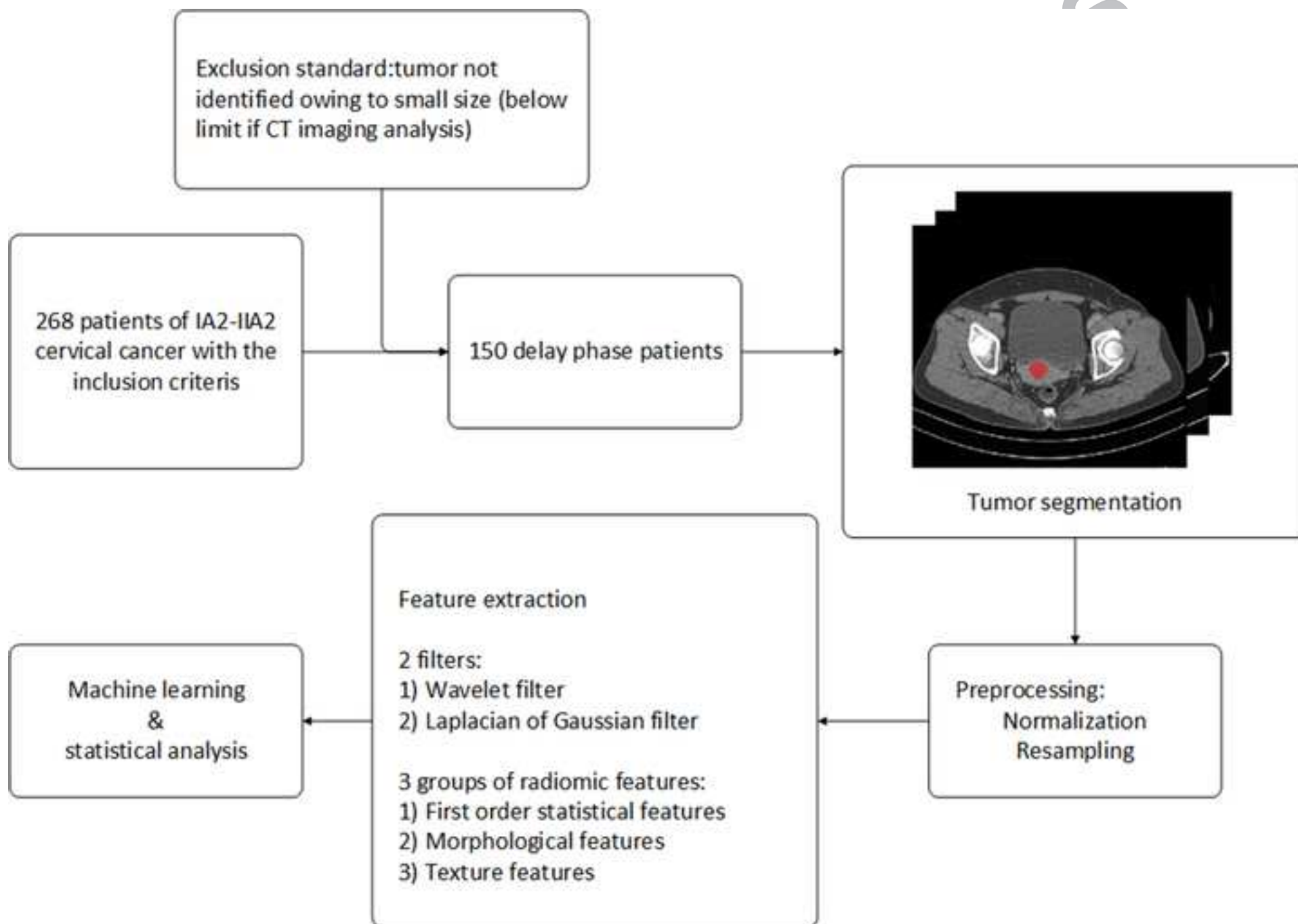
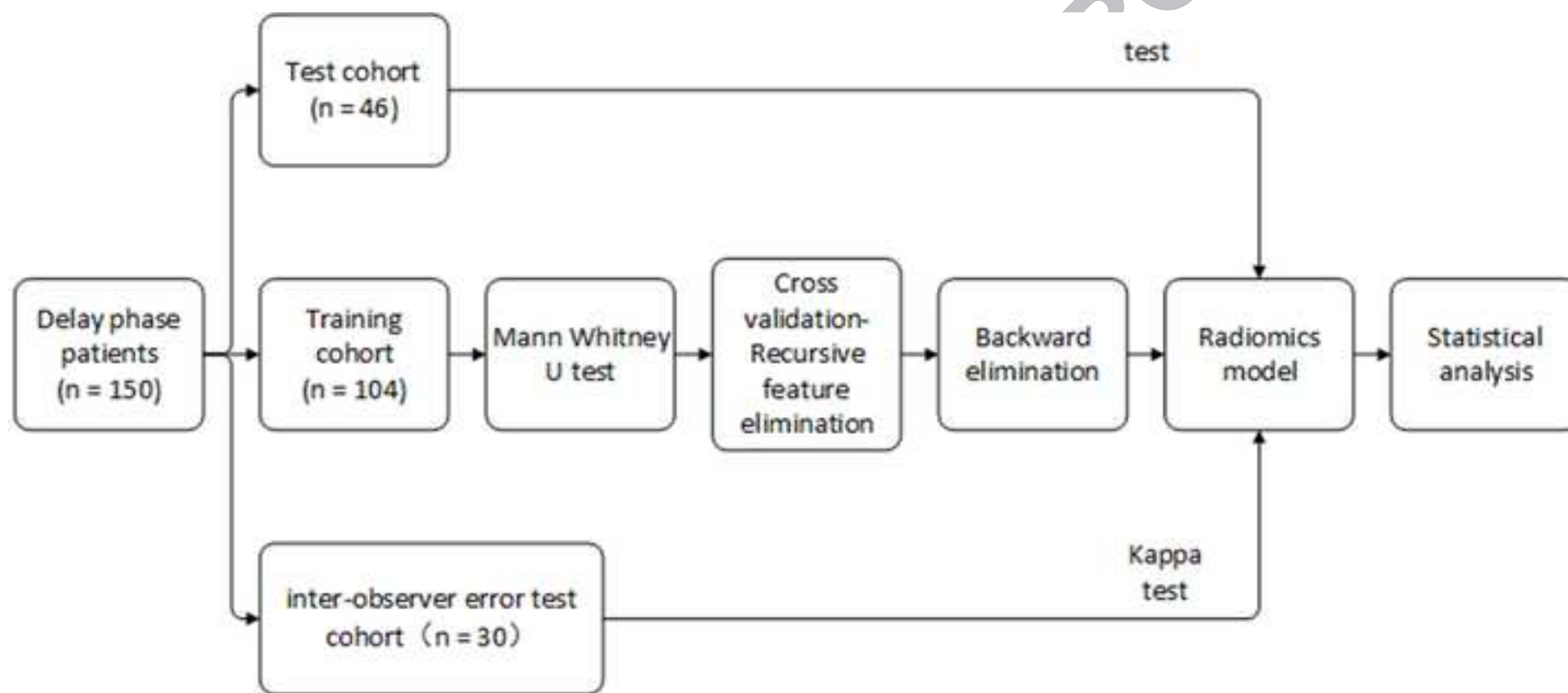
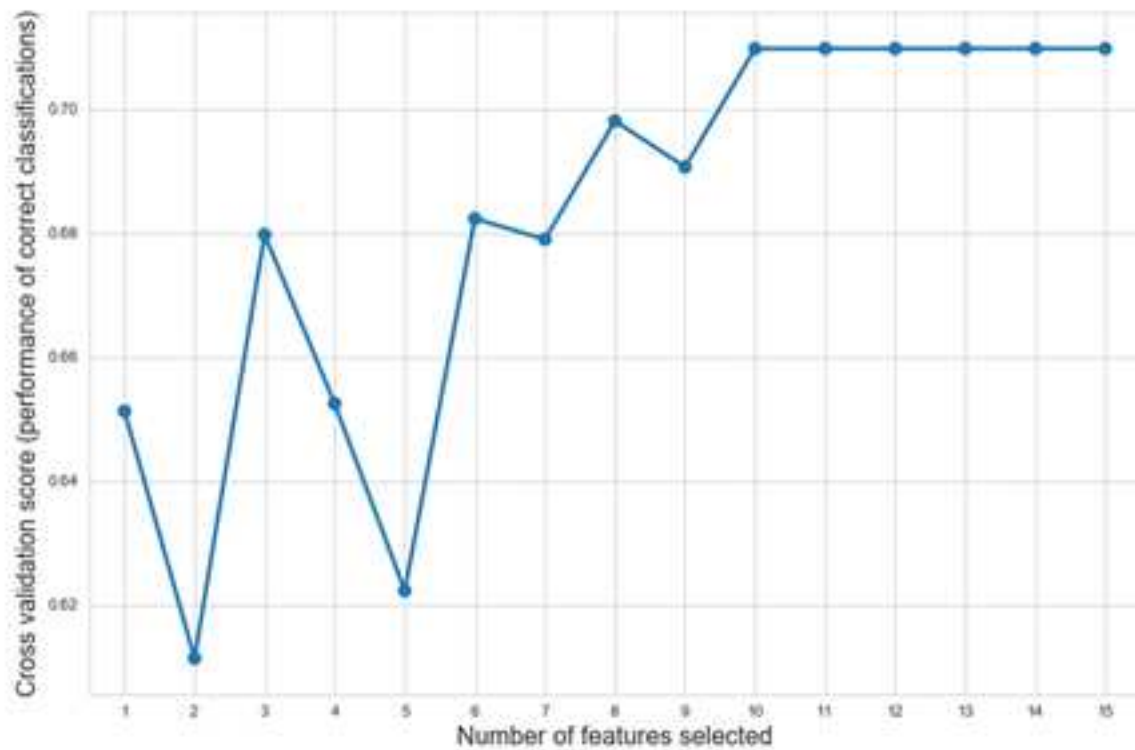


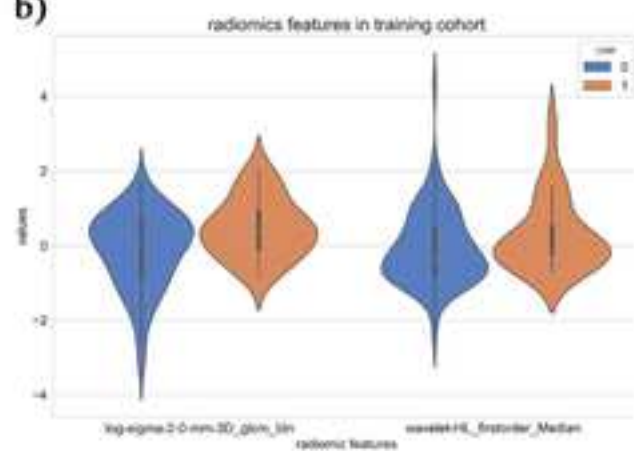
Figure 2



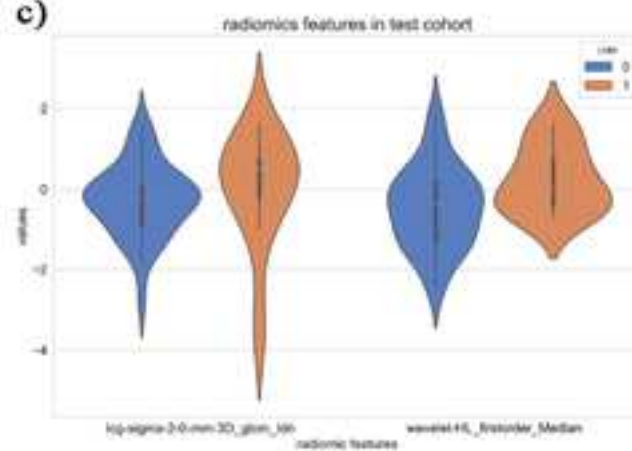
a)



b)



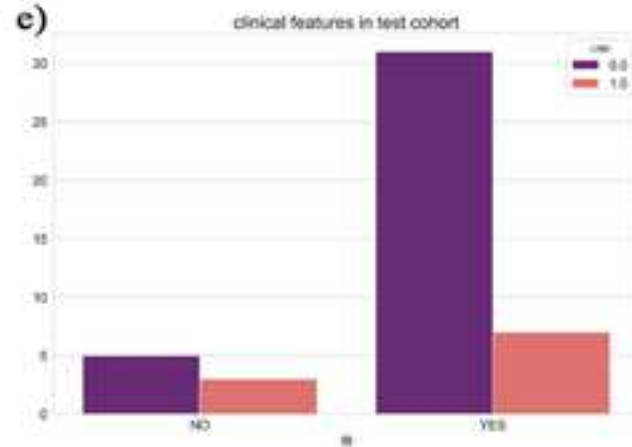
c)



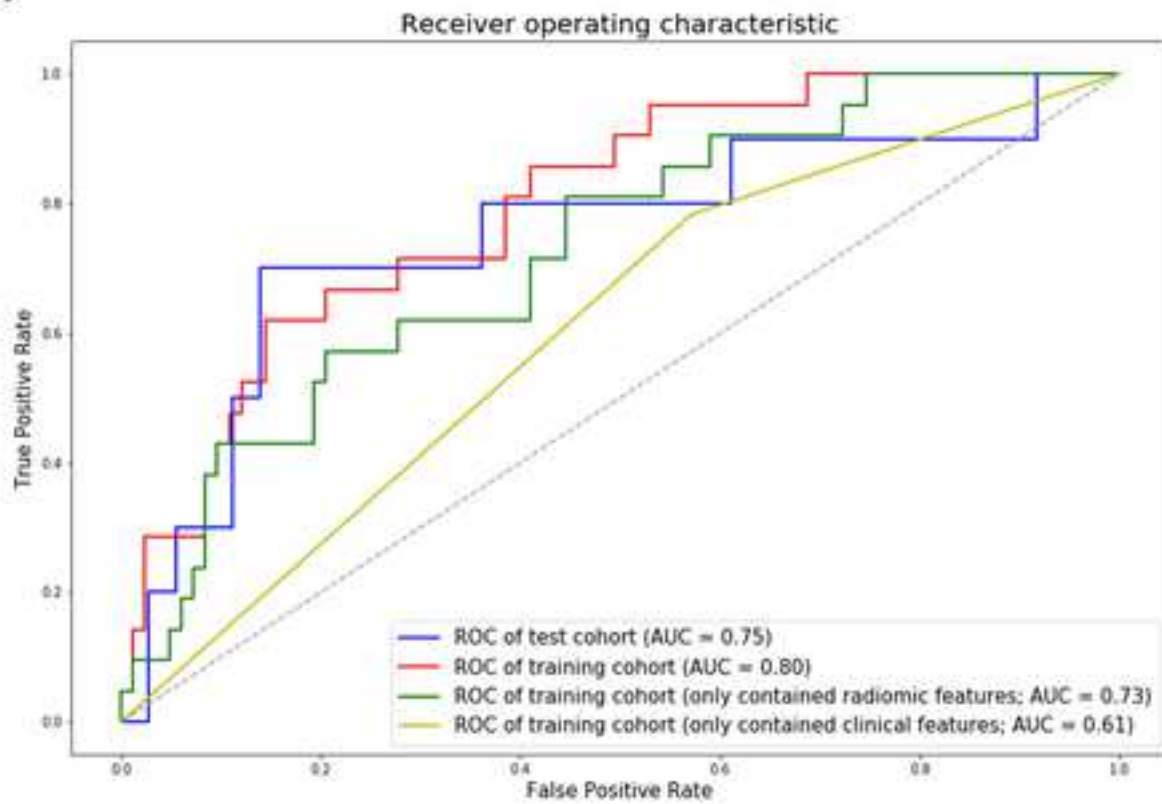
d)



e)



a)



b)

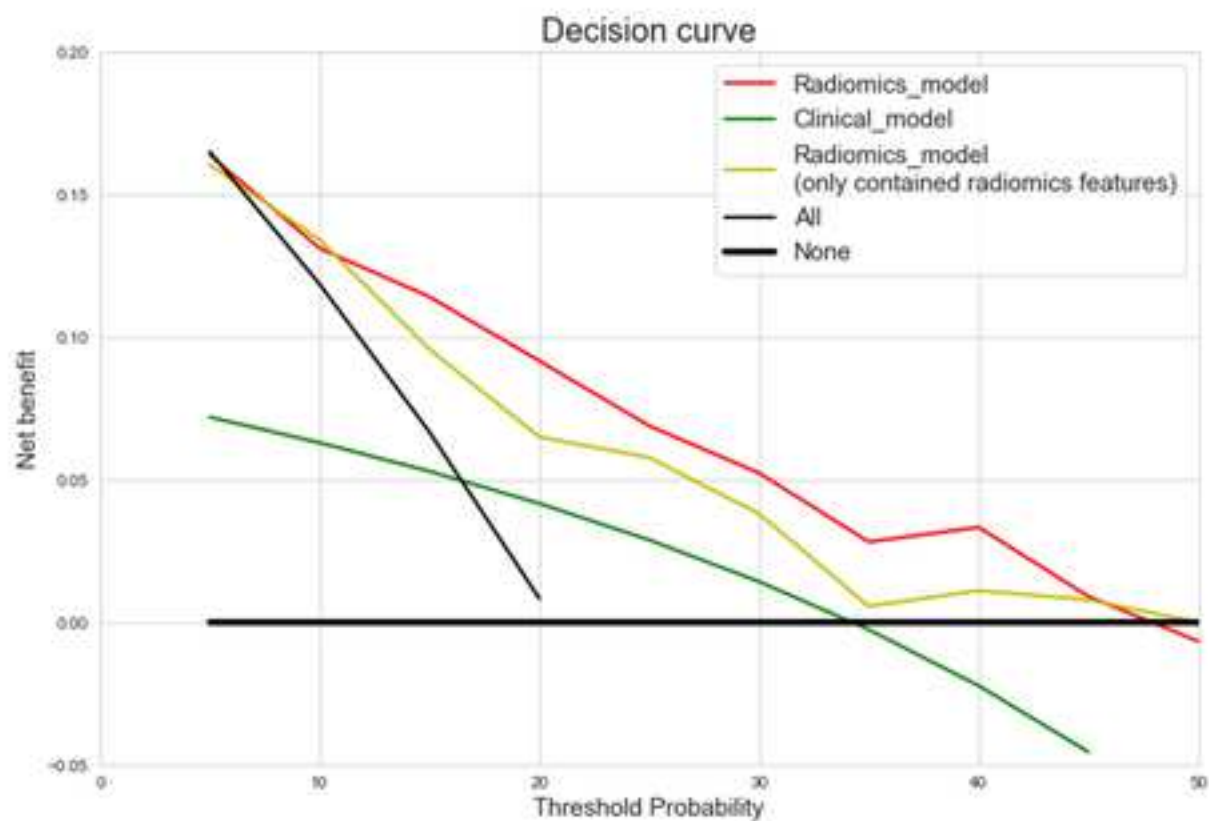


Table 1. Clinical features of patients

Feature	Training cohort		Test cohort		<i>P</i>
	No.	Mean±SD	No.	Mean±SD	
Age		47.87±10.61		45.80±13.72	0.499
FIGO stage					< 0.001*
IB	77		38		
IIA	27		8		
Pregnancy		3.77±2.00		3.76±1.92	0.1155
Histologic type					0.3996
Squamous carcinoma	82		38		
Non-squamous carcinoma	21		6		
Parturition		2.77±1.47		2.43±1.47	0.1319
Menarche time		14.26±2.76		13.70±3.78	0.0537
CT-reported LN status					0.1445
Negative	84		39		
Positive	15		5		
CT-reported vagina status					0.1464
Negative	96		42		
Positive	3		2		
CT-reported uterus status					0.4678
Negative	97		37		
Positive	2		7		

NOTE: *P* value was calculated from univariable analysis between each of the clinical features and LN status. **P* value < 0.05

Click here to access/download
Supplementary material
Supplement 1.docx